Supporting Information

Amphiphilic electrolyte additive as ion-flow stabilizer enables superb zinc metal batteries

Zimin Yang, [a,c] Yilun Sun, [a] Siting Deng, [a,e] Hao Tong, [a,c] Mingqiang Wu, [a,e] Xinbin Nie, [b] Yifan Su, [b] Guanjie He, [d] Yinghe Zhang, [f] Jianwei Li,[*b] Guoliang Chai[*a,g]

a. State Key Laboratory of Structural Chemistry, Fujian Institute of Research on the Structure of Matter, Chinese Academy of Sciences, Fuzhou, 350002 Fujian, P. R. China.

b. Key Laboratory of Comprehensive and Highly Efficient Utilization of Salt Lake Resources, Qinghai Province Key Laboratory of Resources and Chemistry of Salt Lakes, Qinghai Institute of Salt Lakes, Chinese Academy of Sciences, Xining, Qinghai 810008, P. R. China.

c. College of Chemistry and Materials Science, Fujian Normal University, Fuzhou 350007, Fujian, P. R. China.

d. Electrochemical Innovation Lab, Department of Chemical Engineering, University College London, Torrington Place, London WC1E 7JE, U.K.

e. College of Chemistry, Fuzhou University, Fuzhou 350108, China

f. Shenzhen Key Laboratory of Advanced Functional Carbon Materials Research and Comprehensive Application, School of Science, Harbin Institute of Technology, Shenzhen 518055, China

g. School of Chemical Science, University of Chinese Academy of Sciences, Beijing 100049, China.

*Corresponding author. E-mail: jianwei.li@isl.ac.cn; g.chai@fjirsm.ac.cn

Experimental Section

Materials

3-(Hydroxy (phenyl) phosphoryl) propanoic acid (HPA, powder) was purchased from TCI. $Zn(OTf)_2$ was purchased from TCI. MnO_2 was purchased from Macklin. Zinc foils and Cu foils were purchased from Guangdong Ares Metal Technology Co. Ltd. Zinc foils (0.07mm thickness, 99.999% purity) and Cu foils (0.05mm thickness, 99.99% purity) were purchased from Guangdong Ares Metal Technology Co. Ltd.

Fabrication of electrolytes

Aqueous electrolytes, formulated with 2M (M: mol/L) $Zn(OTf)_2$ and 2M $Zn(OTf)_2$ with 1mM HPA**,** 5mM HPA, 10 mM HPA**,** and 15 mM HPA, are named BE, HPA1, HPA5, HPA10, and HPA15, respectively.

Characterizations

The Nuclear Magnetic Resonance (NMR, JEOL ECZ400S, Japan), and Fourier transform infrared (FTIR, Thermo Nicolet iS50) were employed to analyze the element and surface chemistry of the samples. Zn foils were characterized with X-ray diffraction (XRD, MiniFlex 600, Cu-K_α radiation), Scanning Electron Microscopy (SEM, Hitachi SU-8010), and X-ray photoelectron spectroscopy (XPS, ESCALAB 250Xi spectrophotometer with Al-K radiation system). The *in-situ* optical microscope images were obtained on an electron microscope (XJ-906H, Shenzhen Xianjian Juye Electronics Co. Ltd., China) by using a homemade *in-situ* optical electrochemical cell. The SAXS data was obtained by the small-angle X-ray scattering instrument (Xeuss 3.0). The X-ray absorption fine structure analysis (XAFS) experiment described in this paper was performed at the Shanghai Synchrotron Radiation Facility.

Electrochemical Measurements

Zn plating/stripping properties of Zn symmetric batteries and electrochemical performance of full batteries were performed with LIR2025 coin-type cells. The performance of coin-type cells was recorded on NEWARE battery-testing instrument (CT-4008Tn-5V10/20/50mA/1A, Shenzhen, China) at room temperature. The cathode was fabricated by mixing the commercial MnO_2 powder, super P, and polyvinylidene fluoride (PVDF) with a weight ratio of 7:2:1 using N-methyl-2-pyrrolidone (NMP) as solvent. The mixture slurry was printed on hydrophilic carbon paper and then transferred to a vacuum oven drying under 60℃ for 12 h. Finally, cathodes were prepared by cutting circular discs from the dried samples. The loading mass of cut disk of electrodes are all within the scope of 2~2.5 mg along with a diameter of 1.2 cm. Zinc foil and Whatman GF/C glass microfiber were employed as the anode and separator, respectively. The volume of electrolytes in each coin cell is 0.08ml. Each pouch-type Zn//Zn symmetric cell consisted of two 3×3 cm^2 Zn foils as electrodes and two 3×3.1 cm^2 glass fiber separator**s**. Each pouch-type Zn/Cu cell consisted of one 3×3 cm^2 Zn foil and one 3×3 cm^2 Cu foil as electrodes and two 3×3.1 cm^2 glass fiber separators. The shell of the pouch cell was an aluminum–plastic film and the amount of electrolyte was 0.6 mL. Linear sweep voltammetry (LSV), cyclic voltammetry (CV), chronoamperometry (CA), and electrochemical impedance spectroscopy (EIS) were performed using an electrochemical workstation (CHI760E, Shanghai, China). The LSV test was conducted using a three-electrode system, with Ag/AgCl electrode, glass carbon electrode, and Ti anode serving as the reference, counter, and working electrodes,

respectively. CV curves of Zn plating/stripping using Ti as the working electrode and Zn as the reference and counter electrode. CA plots were carried out with Zn symmetric batteries (coin-type cells) at an overpotential of -150 mV and a duration of 400 s.

The transference number of (t_{Zn}^{2+}) was calculated by the following equation (the typical Evans method):

$$t_{Zn^{2+}} = \frac{I_s(\Delta V - I_0 R_0)}{I_0(\Delta V - I_S R_S)} \quad \text{(S1)}$$

Where ΔV is the applied polarization voltage (15 mV), I_0 and R_0 are the initial current and resistance. I_s and R_s are the steady-state current and resistance, respectively.

Computational Methods

The calculations of the binding energies, HOMO and LUMO were performed with Gaussian 16 program[1]. The geometric structure of the molecules and ions were calculated by M06-2X[2] method with a basis set aug-cc-pVTZ.[3] The vibrational frequencies and thermal correction to Gibbs free energy of the molecules and ions were calculated at optimized geometry using the same level of theory. The energies of binding energies are Gibbs free energies. The electrostatic potential (ESP) was created by GaussView 6.0 from total SCF density. The method and basis set used in the calculation are identical to those mentioned above.

The first-principles DFT calculations of adsorption energies were performed using the Vienna *Ab initio* Simulation Package (VASP) code.[4] All the calculations were carried out by using Perdew−Burke−Ernzerh (PBE) for exchange−correlation functional. The spin-polarized Kohn−Sham equations were solved in the plane-wave and pseudopotential framework with a cutoff of 500 eV.

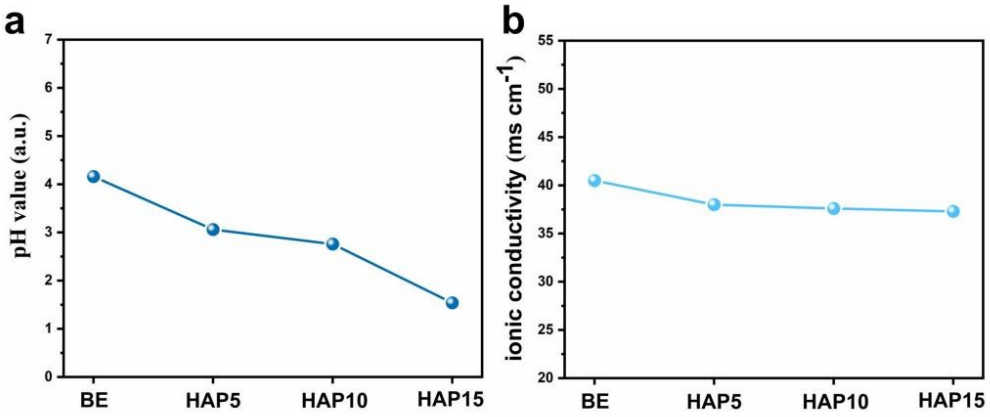

Fig.S1 Measured pH and ionic conductivity of different electrolytes.

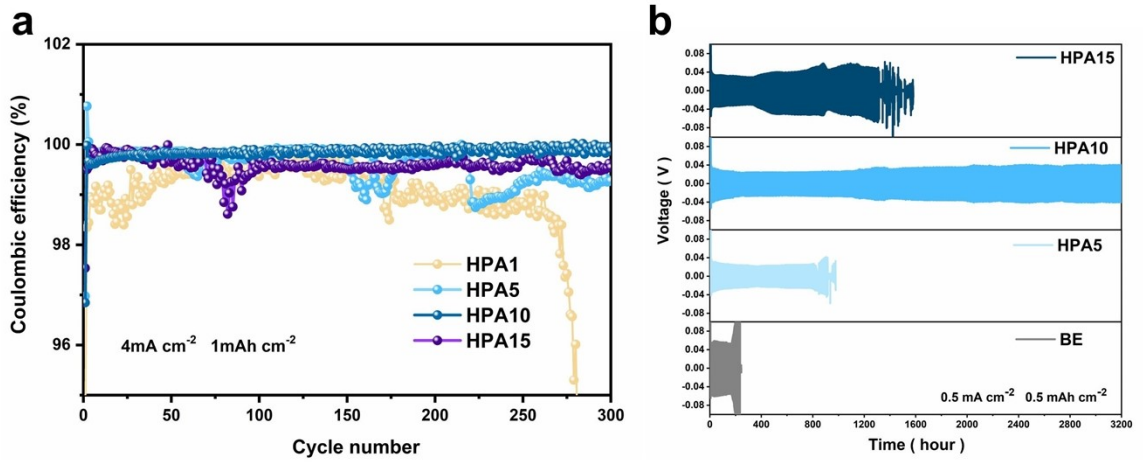

Fig. S2 (a) Coulombic efficiency of Zn/Cu cells in electrolytes with different content of HPA additives; (b) Long-term galvanostatic Zn stripping/plating in the Zn/Zn symmetric cells with different electrolytes under 0.5 mA cm^{-2}, 0.5 mAh cm^{-2}.

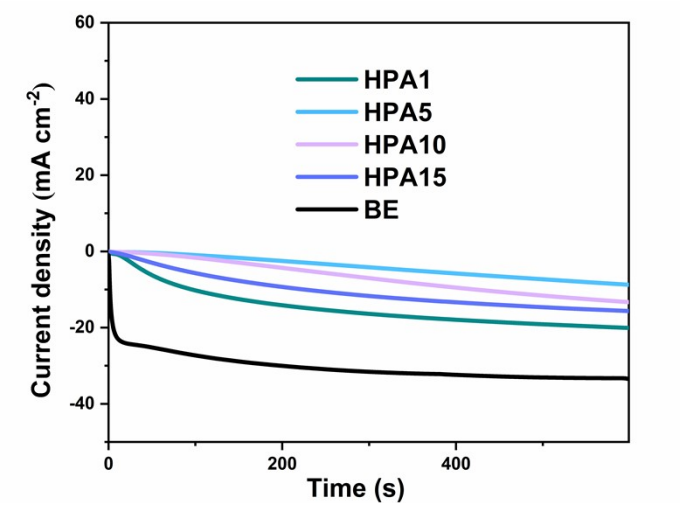

Fig. S3 Chronoamperometry curves of Zn//Zn symmetric cells with different electrolytes.

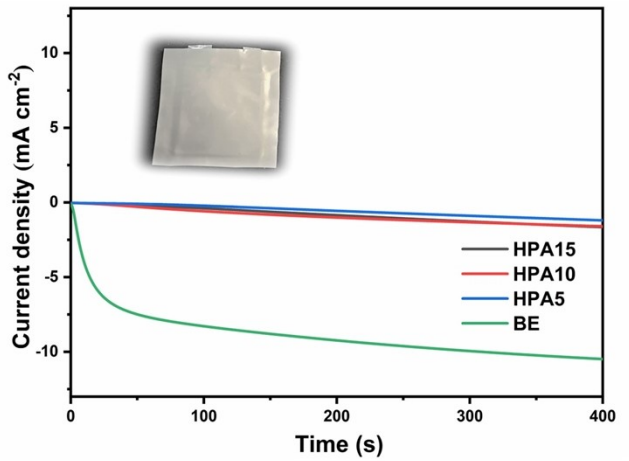

Fig. S4. Chronoamperometry curves of Zn//Zn symmetric pouch cells with different content of HPA additives (the insert image is the pouch cell).

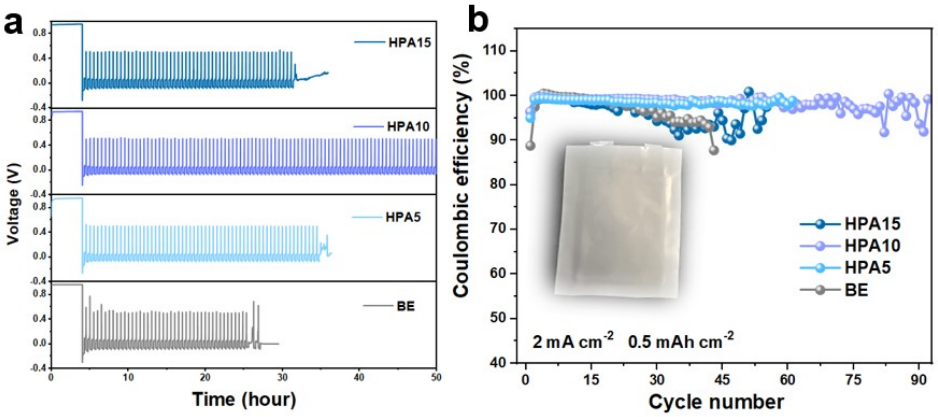

Fig. S5 (a) The voltage-time curve of Zn//Cu pouch cells in electrolytes with different content of HPA additives; (b) Coulombic efficiency of Zn/Cu pouch cells in electrolytes with different content of HPA additives.

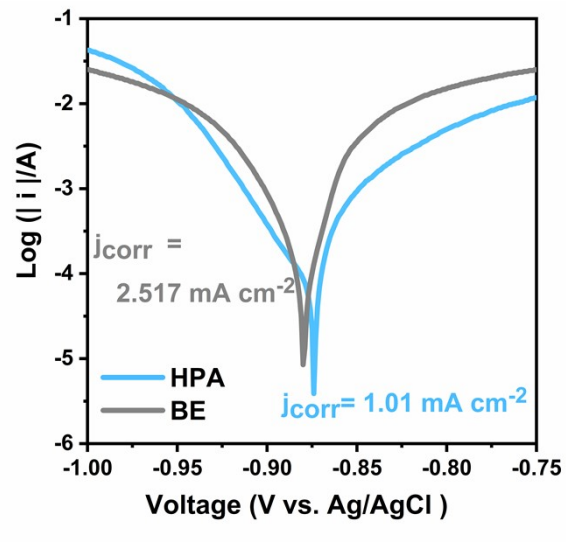

Fig. S6 Linear polarization curves for describing corrosion of Zn anodes in different electrolytes.

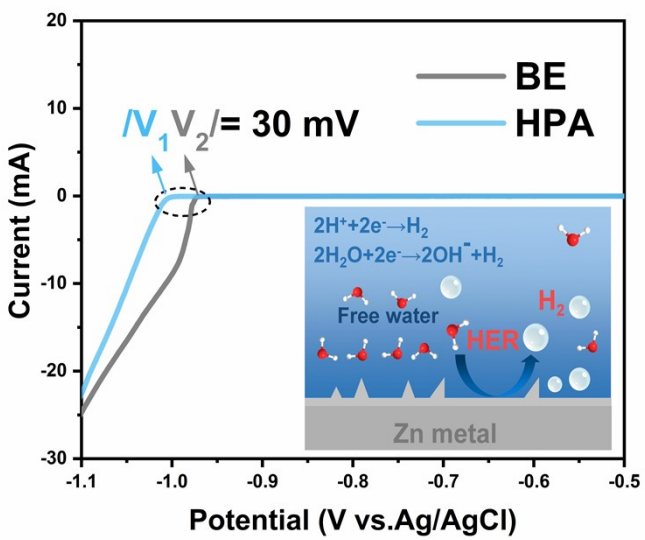

Fig. S7 The linear sweep voltammetry (LSV) curves of various electrolytes.

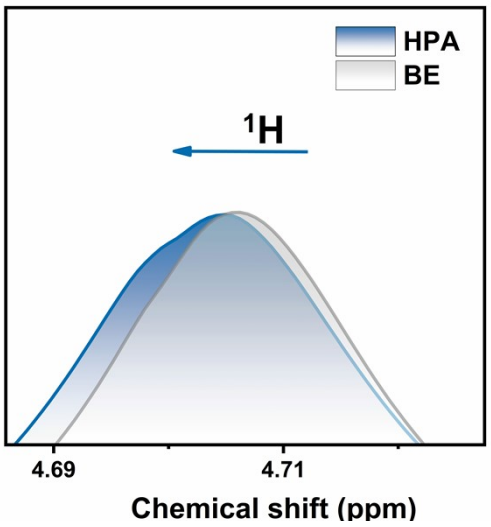

Fig. S8 ^{1}H NMR of the different electrolytes.

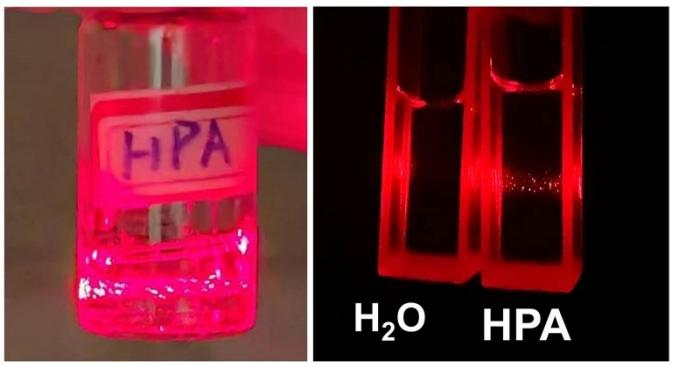

Fig. S9 Tyndall effect of the HPA electrolytes and H_2O.

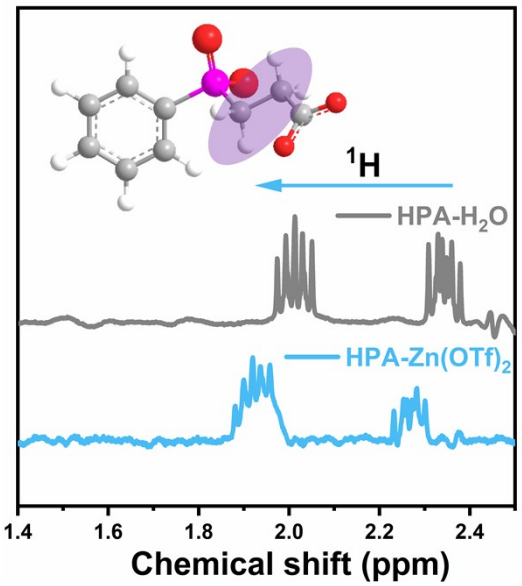

Fig. S10 ^{1}H NMR of the different electrolytes.

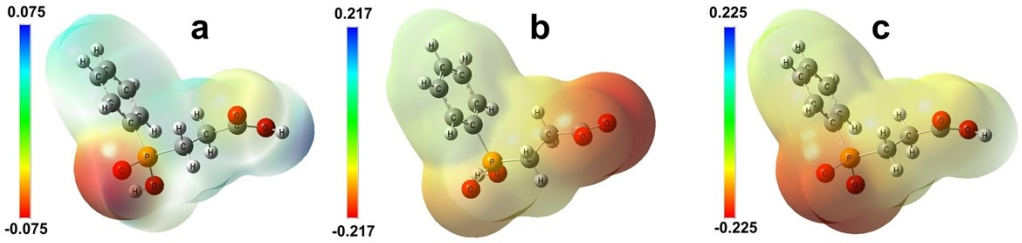

Fig. S11 The electrostatic potential (ESP) plots of (a) HPA, (b) HPA with COO^-, and (c) HPA with PO^-.

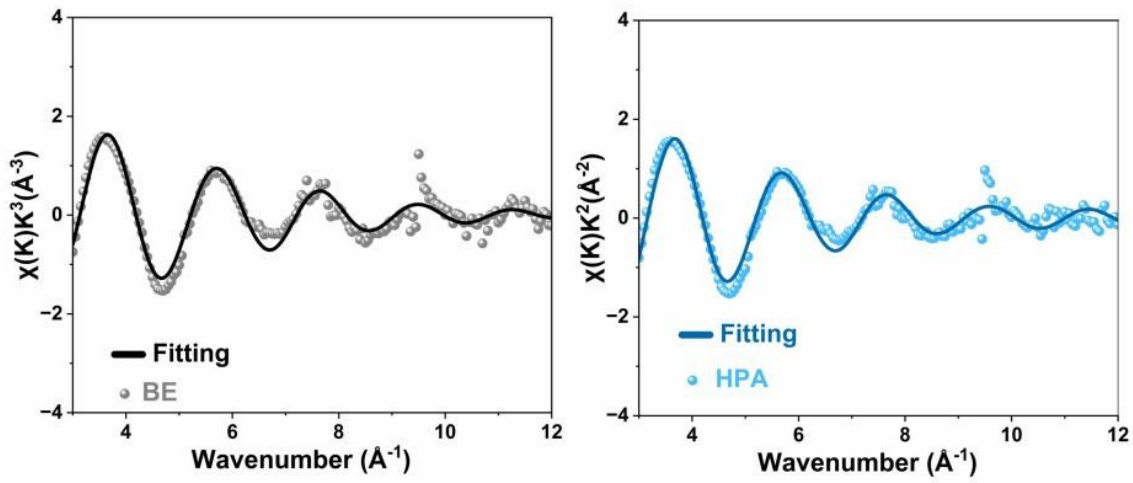

Fig.S12 k^3/k^2-weighted Fourier transform of Zn K-edge EXAFS spectra of different electrolytes in the k-space.

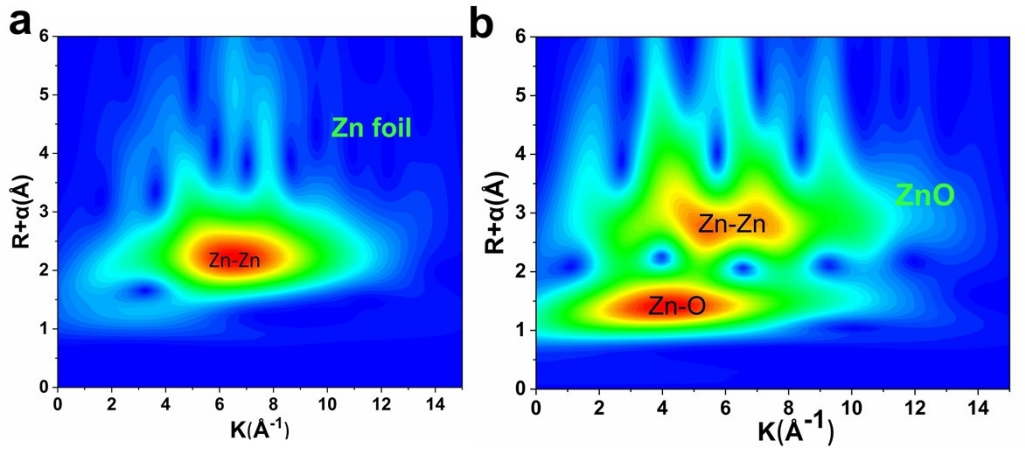

Fig. S13 Wavelet transform images of the EXAFS spectra for Zn foil and ZnO.

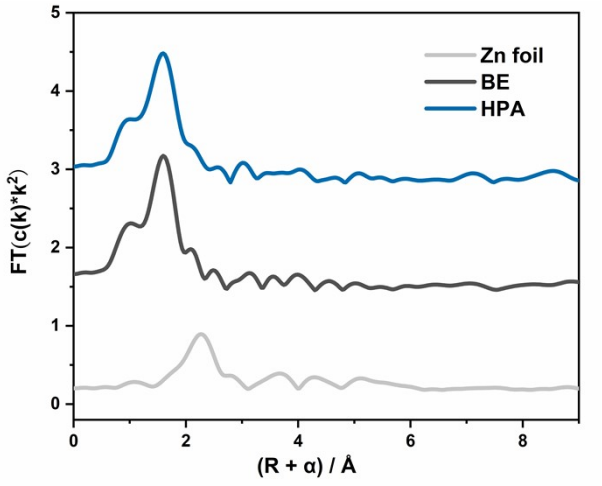

Fig. S14 Comparison between experimental Zn K-edge XANES spectra of Zn foil and different electrolytes.

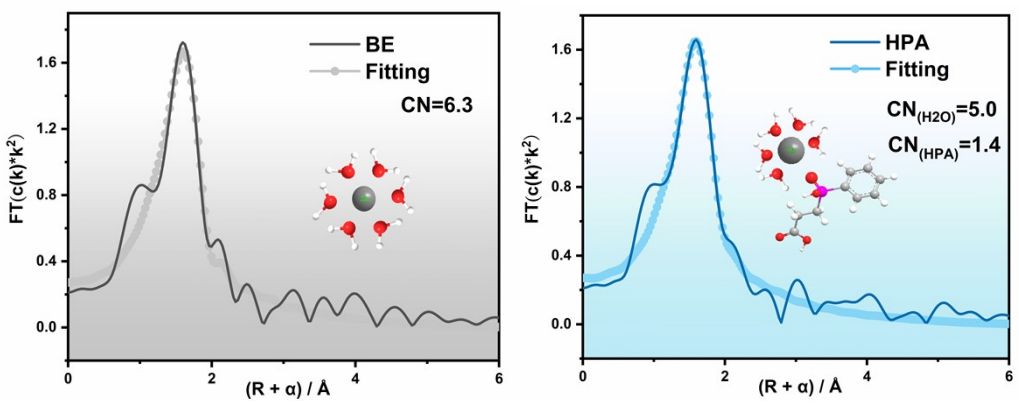

Fig. S15 FT-EXAFS fitting curves at R space of different electrolytes (CN: coordination numbers).

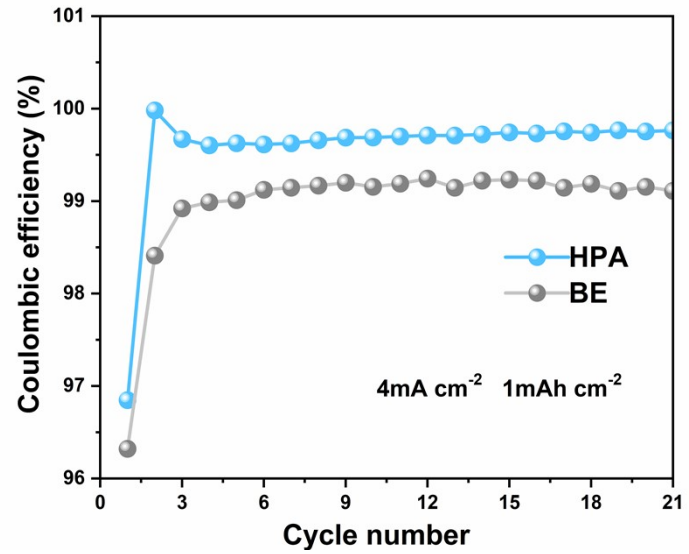

Fig.S16 CE and cycling performance of Zn//Cu cells at a current density of 4 mA cm^{-2} with 1 mAh cm^{-2}.

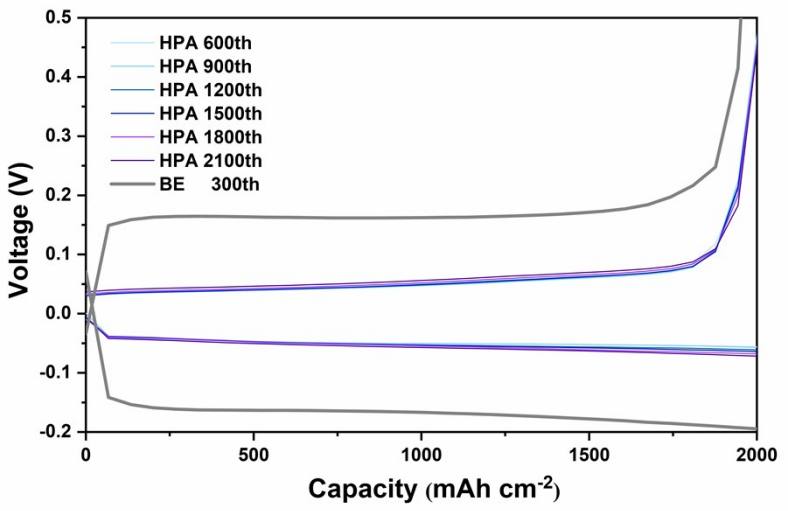

Fig. S17 Voltage profiles of Zn//Cu cells in electrolytes with/without HPA additive.

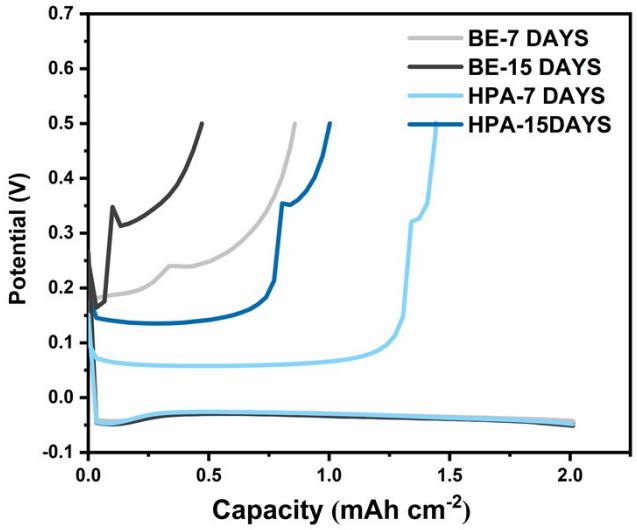

Fig. S18 The corresponding voltage profiles of cells aged for 7/15 days in electrolytes with/without HPA.

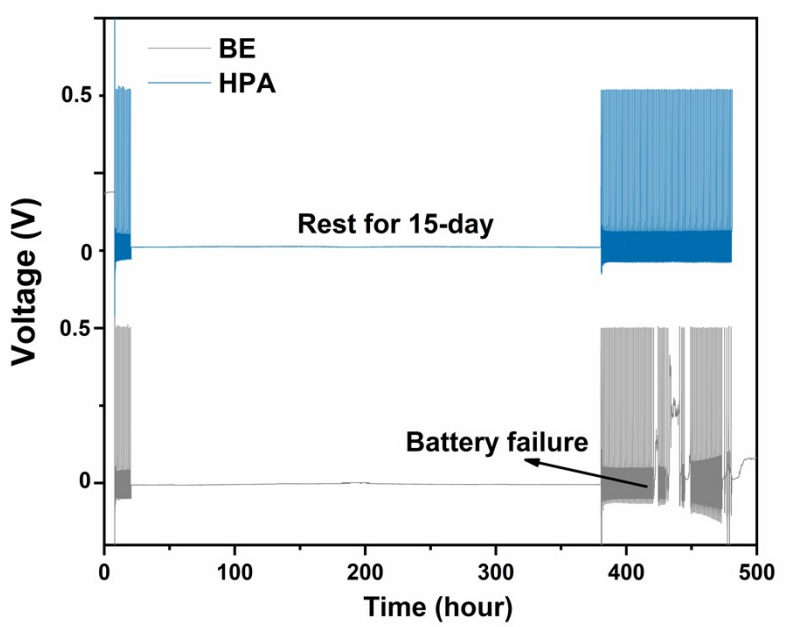

Fig. S19 Potential curve of Zn/Cu cells with different electrolytes.

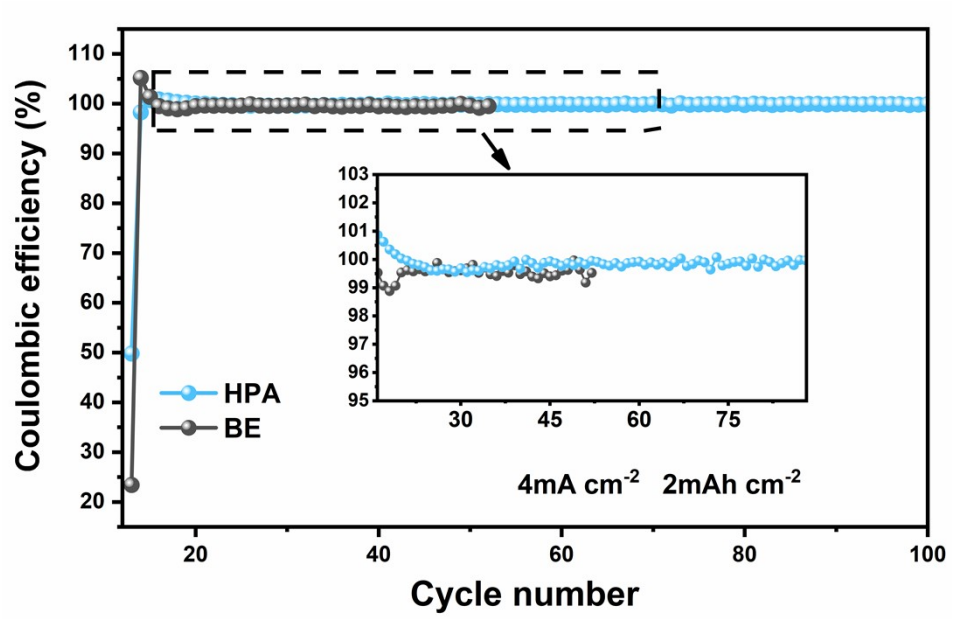

Fig. S20 CE of Zn//Cu cells using electrolytes with/without HPA after the process of 15-day aging.

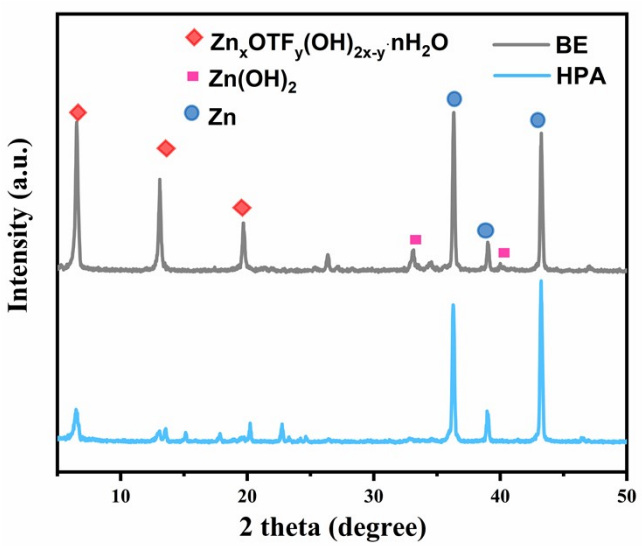

Fig. S21 XRD patterns of Zn foils after soaking in different electrolytes for 30 days.

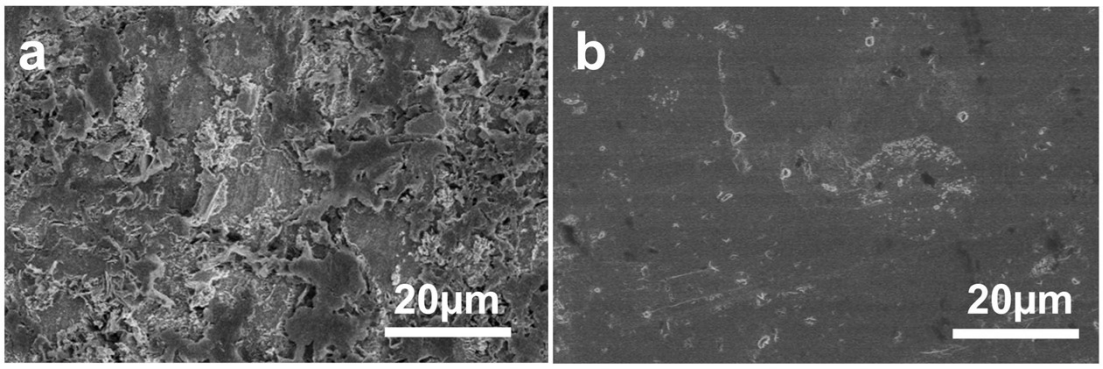

Fig. S22 The images of Zn anodes in a) $Zn(OTf)_2$ electrolyte and b) HPA/$Zn(OTf)_2$ electrolyte after cycling for 100 h.

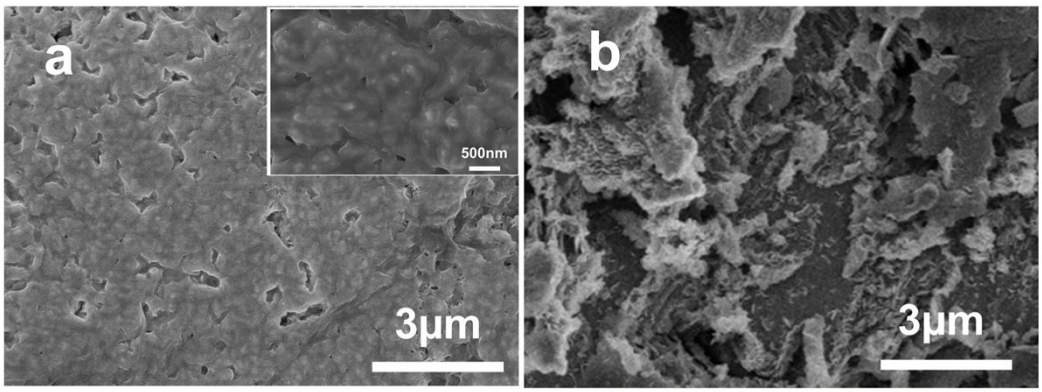

Fig. S23 The images of Zn anodes in a) HPA/$Zn(OTf)_2$ electrolyte and b) $Zn(OTf)_2$ electrolyte after cycling for 50 h.

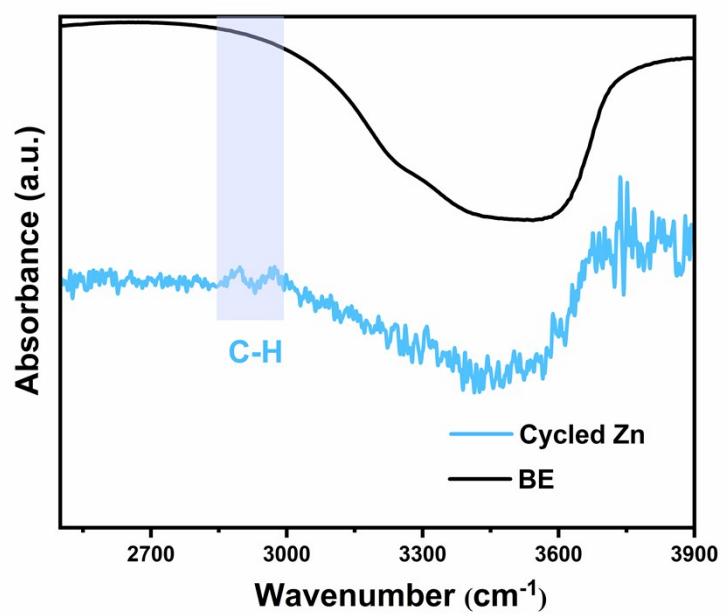

Fig. S24 FTIR spectra of the $Zn(OTf)_2$ electrolyte and cycled Zn anode.

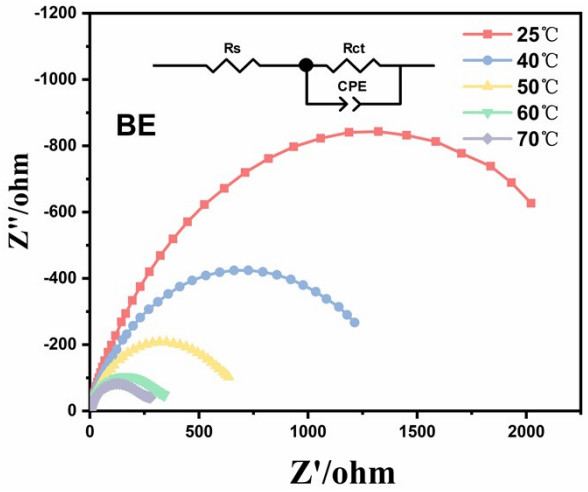

Fig. S25 Nyquist plots at different temperatures for Zn//Zn symmetrical batteries in pure $Zn(OTf)_2$ electrolyte (the insert picture is the fitting circuit of symmetric batteries).

The Arrhenius activation energy (E_a) can be approximated as the desolvation energy barrier for hydrated Zn^{2+}, which can be calculated according to the following Arrhenius equation[5, 6]:

$$1/R_{ct} = A \exp (E_a/RT) \quad (S2)$$

where R_{ct}, A, R, and T represent the charge-transfer resistance, the frequency factor, the gas constant, and the absolute temperature, respectively.

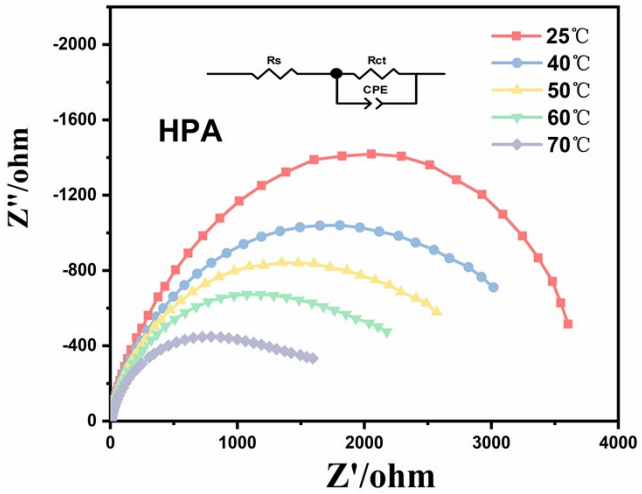

Fig. S26 Nyquist plots at different temperatures for Zn//Zn symmetrical batteries in HPA/$Zn(OTf)_2$ electrolyte (the insert picture is the fitting circuit of symmetric batteries).

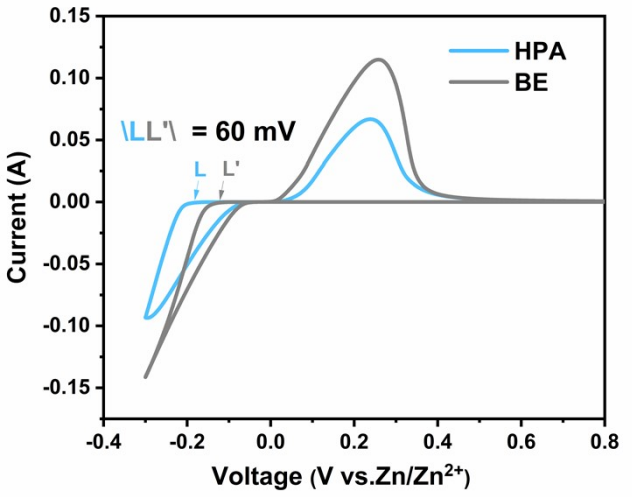

Fig. S27 CV curves of Zn/Ti cells in electrolytes with/without HPA additive.

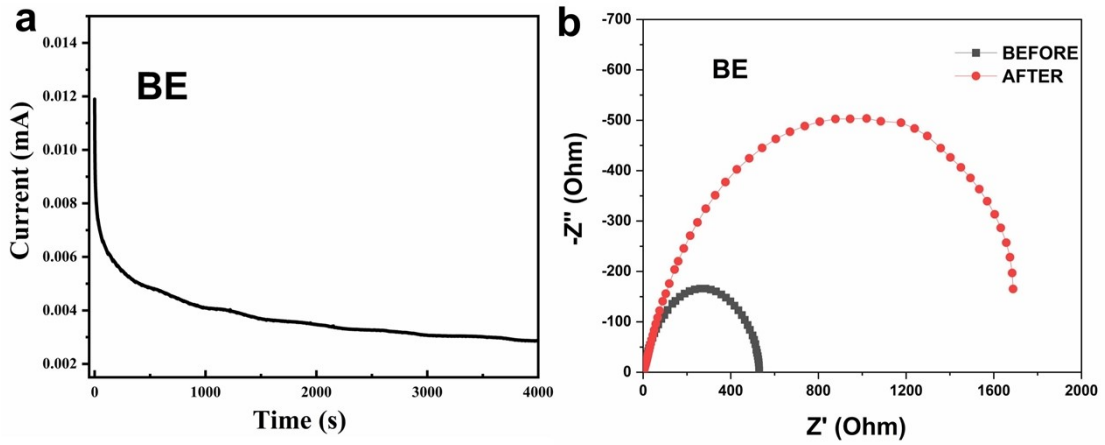

Fig. S28 (a) Current-time plots of Zn//Zn symmetric cells with $Zn(OTf)_2$ electrolyte after polarization at a constant potential (15 mV) for 4000 s; (b) The impedance spectra before and after polarization.

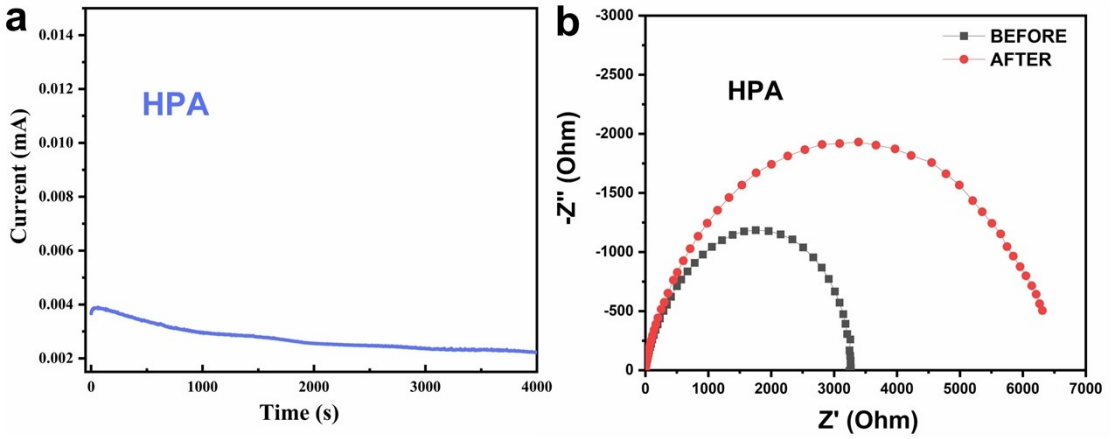

Fig. S29 (a) Current-time plots of Zn symmetric cells with HPA/Zn(OTf)$_2$ electrolyte after polarization at a constant potential (15 mV) for 4000 s; (b) The impedance spectra before and after polarization.

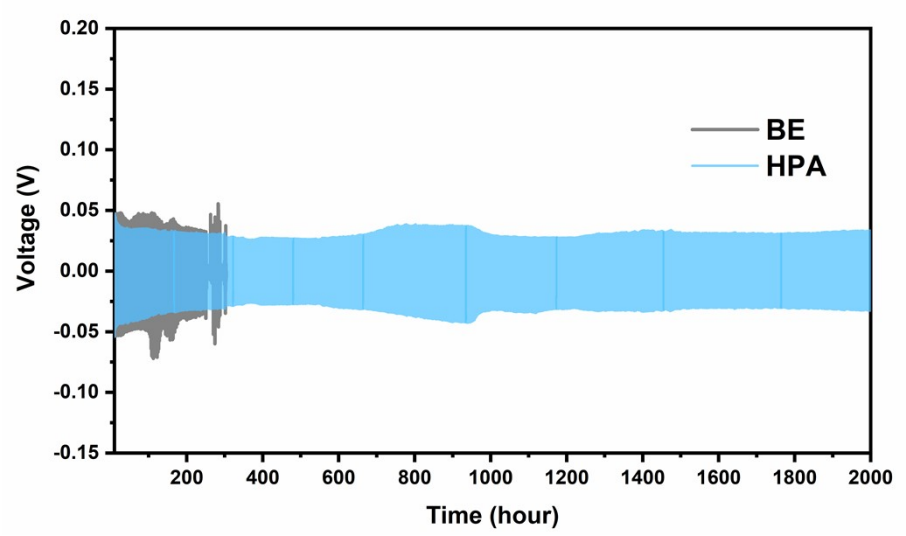

Fig. S30 Reproduced test of long-term galvanostatic Zn stripping/plating in the Zn/Zn symmetric cells under 0.5 mA cm^{-2}, 0.5 mAh cm^{-2}.

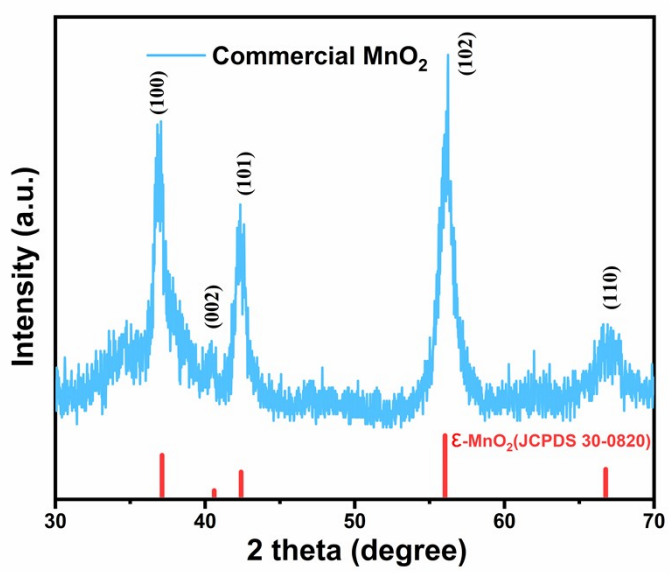

Fig. S31 XRD patterns of commercial MnO_2 powder.

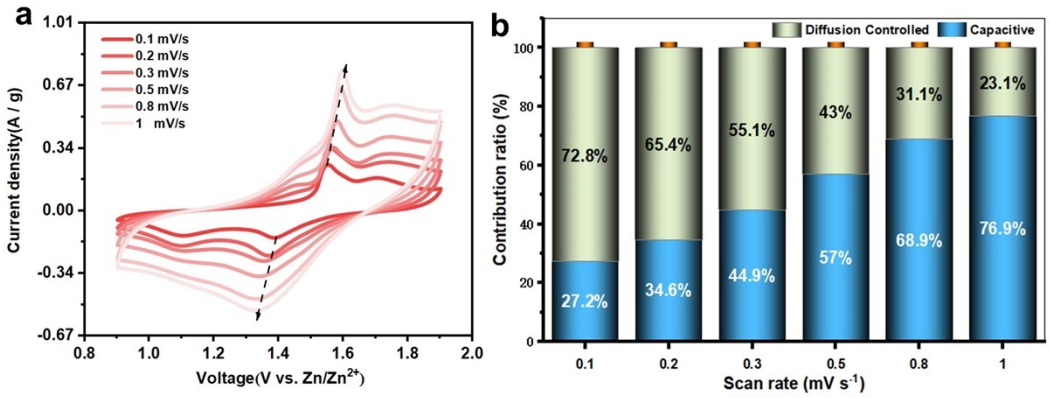

Fig. S32. (a) CV profiles of the Zn//MnO_2 battery with HPA from 0.1 to 1 mV s^{-1}; (b) Contribution ratio of the capacitive capacities and diffusion-limited capacities at different scan rates.

In principle, electrochemical kinetics can be analyzed via power-law formula as $i = av^b$, where i is the current (A), a and b are variable parameters and v is the scan rate (V/s). In general, the value b represents the type of electrochemical charge storage reaction.

The power-law formula $i = av^b$ can be divided into two parts to quantify the capacitive (k_1v) and diffusion ($k_2v^{1/2}$) contributions:

$$i = k_1v + k_2v^{1/2} \quad \text{(S3)}$$

Table S1. Fitting results of EXAFS of different samples

Sample	Path	CN	R(Å)	$\sigma^2(10^{-3}Å^2)$	ΔE_0(eV)	R factor
BE	Zn-O	6.3	2.07	7.8	0.357	0.024
HPA	Zn-O (P)	1.4	2.00	2.5	0.869	0.008
	Zn-O (H_2O)	5.0	2.10	7.6	0.869	0.008

CN: coordination numbers; R: bond distance; σ^2: Debye-Waller factors; ΔE_0: the inner potential correction; R factor: goodness of fit. S_0^2 was set as 0.96. The data ranges are presented as $3 \leq k \leq 12.269$ $Å^{-1}$, $1 \leq R \leq 2.6$ Å for BE; $3 \leq k \leq 12.27$ $Å^{-1}$, $1 \leq R \leq 2.6$ Å for HPA. Error bounds that characterize the structural parameters obtained by EXAFS spectroscopy were estimated as CN ± 20%: σ^2 ± 20%: R ± 0.03 Å.

References

[1] Risch, M. J.; Trucks, G. W.; Schlegel, H. B.; Scuseria, G. E.; Robb, M. A.; Cheeseman, J. R.; Scalmani, G.; Barone, V.; Petersson, G. A.; Nakatsuji, H.; Li, X.; Caricato, M.; Marenich, A.V; Bloino, J.; Janesko, B. G.; Gomperts, R.; Mennucci, B.; Hratchian, H. P.; Ortiz, J.V; Izmaylov, A. F.; Sonnenberg, J. L.; Williams-Young, D.; Ding, F.; Lipparini, F.; Egidi, F.; Goings, J.; Peng, B.; Petrone, A.; Henderson, T.; Ranasinghe, D.; Zakrzewski, V. G.; Gao, J.; Rega, N.; Zheng, G.; Liang, W.; Hada, M.; Ehara, M.; Toyota, K.; Fukuda, R.; Hasegawa, J.; Ishida, M.; Nakajima, T.; Honda, Y.; Kitao, O.; Nakai, H.; Vreven, T.; Throssell, K.; Montgomery Jr., J. A.; Peralta, J. E.; Ogliaro, F.; Bearpark, M. J.; Heyd, J. J.; Brothers, E. N.; Kudin, K. N.; Staroverov, V. N.; Keith, T. A.; Kobayashi, R.; Normand, J.; Raghavachari, K.; Rendell, A. P.; Burant, J. C.; Iyengar, S. S.; Tomasi, J.; Cossi, M.; Millam, J. M.; Klene, M.; Adamo, C.; Cammi, R.; Ochterski, J. W.; Martin, R. L.; Morokuma, K.; Farkas, O.; Foresman, J. B.; Fox, D. J. Gaussian16 Revision B.01. 2016.

[2] Y. Zhao, D. G. Truhlar, *Theor. Chem. Acc.* 2008, **120**, 215-241.

[3] a) T. H. Dunning, Jr., *J. Chem. Phys.* 1989, **90**, 1007-1023; b) R. A. Kendall, T. H. Dunning, Jr., R. J. Harrison, *J. Chem. Phys.* 1992, **96**, 6796-6806.

[4] a) G. Kresse, J. Hafner, *Phys. Rev. B.* 1994, **49**, 14251-14269; b) G. Kresse, J. Furthmüller, *Comp. Mater. Sci.* 1996, **6**, 15-50.

[5] X. Xie, S. Liang, J. Gao, S. Guo, J. Guo, C. Wang, G. Xu, X. Wu, G. Chen and J. Zhou, *Energy Environ. Sci*., 2020, **13**, 503-510.

[6] X. Yang, C. Li, Z. Sun, S. Yang, Z. Shi, R. Huang, B. Liu, S. Li, Y. Wu, M. Wang, Y. Su, S. Dou and J. Sun, *Adv. Mater.*, 2021, **33**, 2105951.